

# A Simplified and Optimized Chemical Mechanism for Combustion of n-Pentane at Atmospheric Pressure

## Authors:

Zhiqun Meng, Jinggang Wang, Jiawen Qi, Chuchao Xiong, Liqun Hou, Jinghui Luo

Date Submitted: 2020-11-11

Keywords: atmospheric pressure, combustion, optimized mechanism, simplified mechanism, n-pentane

## Abstract:

In the present study, the detailed mechanism of n-pentane combustion, including 697 species and 3214 reactions, is first simplified to a mechanism with only 26 species and 134 reactions, which is suitable for the pressure of 1 atm, temperatures of 1000–1600 K, and equivalent ratios of 0.5–1.6. However, when the equivalence ratio is 1.0, in the temperature range of 1000–1100 K, compared with the detailed mechanism, the maximum error of the ignition delay time predicted by the simplified mechanism exceeds 20%. Therefore, based on the method of temperature sensitivity analysis, the simplified mechanism is further utilized through reducing the A-factor of  $2\text{HO}_2 = \text{H}_2\text{O}_2 + \text{O}_2$  (?1) and  $2\text{HO}_2 = \text{H}_2\text{O}_2 + \text{O}_2$  (?2) by 10 times. By comparing with the detailed mechanism and predicting the ignition delay time, laminar flame speed, species profile, and extinction residence time, it is found that the optimized mechanism has good accuracy in the applicable range, and is fully capable of simulating the combustion process of light hydrocarbon gas.

Record Type: Published Article

Submitted To: LAPSE (Living Archive for Process Systems Engineering)

Citation (overall record, always the latest version):

LAPSE:2020.1154

Citation (this specific file, latest version):

LAPSE:2020.1154-1

Citation (this specific file, this version):


LAPSE:2020.1154-1v1

DOI of Published Version: <https://doi.org/10.3390/pr8080884>

License: Creative Commons Attribution 4.0 International (CC BY 4.0)

Article

# A Simplified and Optimized Chemical Mechanism for Combustion of *n*-Pentane at Atmospheric Pressure

Zhiqun Meng , Jinggang Wang \*, Jiawen Qi, Chuchao Xiong, Liquan Hou and Jinghui Luo

School of Energy and Environmental Engineering, Hebei University of Engineering, Handan 056038, China; fanzqmeng@163.com (Z.M.); jiawenqi1001@163.com (J.Q.); xiongchuchao@126.com (C.X.); houliquan@sina.com (L.H.); jinghuiluo@126.com (J.L.)

\* Correspondence: jinggangwang@hebeu.edu.cn

Received: 24 June 2020; Accepted: 20 July 2020; Published: 22 July 2020



**Abstract:** In the present study, the detailed mechanism of *n*-pentane combustion, including 697 species and 3214 reactions, is first simplified to a mechanism with only 26 species and 134 reactions, which is suitable for the pressure of 1 atm, temperatures of 1000–1600 K, and equivalent ratios of 0.5–1.6. However, when the equivalence ratio is 1.0, in the temperature range of 1000–1100 K, compared with the detailed mechanism, the maximum error of the ignition delay time predicted by the simplified mechanism exceeds 20%. Therefore, based on the method of temperature sensitivity analysis, the simplified mechanism is further utilized through reducing the A-factor of  $2\text{HO}_2 = \text{H}_2\text{O}_2 + \text{O}_2$  (–1) and  $2\text{HO}_2 = \text{H}_2\text{O}_2 + \text{O}_2$  (–2) by 10 times. By comparing with the detailed mechanism and predicting the ignition delay time, laminar flame speed, species profile, and extinction residence time, it is found that the optimized mechanism has good accuracy in the applicable range, and is fully capable of simulating the combustion process of light hydrocarbon gas.

**Keywords:** *n*-pentane; simplified mechanism; optimized mechanism; combustion; atmospheric pressure

## 1. Introduction

Computational Fluid Dynamics (CFD) has been widely used in analyzing combustion technology and designing combustors. The chemical kinetics mechanism of the specific fuel is necessary for CFD. The current CFD software usually uses a one-step or several-step reaction mechanism to simulate the combustion process, but this kind of kinetic model has narrow scope and low reliability. If the combustion is simulated using a detailed chemical kinetic mechanism, it will face two problems [1]. On one hand, the amount of calculation required is very large. The complex reaction of combustion contains hundreds of materials and reactions. In the numerical simulation process, this amount of calculation exceeds the existing calculation capacity. The second problem related to maintaining the computational stability. The time scales of various substances and their reactions vary greatly, which reduces the rigidity of differential equations and the convergence and stability of computational solutions. Therefore, in order to simulate the combustion process accurately and reliably, it is necessary to simplify the mechanism.

*n*-Pentane is the main component of light hydrocarbon gas, which is widely used in the research of Meng et al. [2]. In order to study the combustion process and characteristics of light hydrocarbon gas by CFD simulation, the detailed chemical kinetic mechanism of *n*-pentane needs to be simplified. The chemical mechanism of *n*-pentane has been studied and improved in the last few years. Knox and Kinnear [3] used gas chromatography to study the initial phase of the slow reaction of gaseous *n*-pentane with oxygen under static conditions at 523–673 K through analysis of the reaction products. Hughes et al. [4] studied the reaction of *n*-pentane with oxygen in the temperature range of 530–553 K,

including the slow oxidation zone and the cold flame zone. Qualitative analysis showed that the relative importance of the various products obtained is consistent with the proposed reaction mechanism. Westbrook et al. [5] used a numerical model and detailed chemical kinetic reaction mechanism to study the oxidation reaction of *n*-pentane in a stirred reactor, including 53 chemical species and 326 basic reactions in a temperature range of 1068–1253 K and at atmospheric pressure. The results showed that the main reaction pathway of *n*-pentane is the extraction of H atoms by OH radicals, followed by the extraction of H atoms by H and O atoms, and the decomposition of single molecules to generate ethyl and *n*-propyl radicals. The oxidation reaction of *n*-pentane in a jet-stirred reactor in a temperature range of 950–1050 K, suitable for a wide range of fuel–oxygen equivalence ratios (0.2–2.0), was studied by Chakir et al. [6]. The results proved that there was a good agreement between the calculated and measured concentrations of the main chemicals. Bugler et al. [7] studied the ignition conditions of three pentane isomers under a wide range of temperatures and pressures, and compared the model simulation results with the experimental results performed with a shock tube. The results showed that the ignition delay time and pressure rise were very consistent in the first and second stage ignition events. Zhukov et al. [8] used a shock tube to determine the ignition delay time in an equivalence ratio of 0.5, temperatures of 867–1534 K, and pressures of 11–530 atm, and studied the effect of mixed pressures on ignition at temperatures of 1000–1100 K. The ignition delay times after reflecting shock waves at pressures of 2 to 20 atm, temperatures of 1100 to 1600 K, and a mixture ratio of 0% to 100% at equivalence ratio of 0.5 were measured by Jiang et al. [9]. The National University of Ireland (NUI), Galway pentane isomer model provides a good prediction of the ignition delay time of dimethyl ether, *n*-pentane, and their blends. In a wide range of equivalence ratios, at atmospheric pressure, and elevated unburned mixture temperatures, Ji et al. [10] measured the laminar flame speeds and extinction strain rates of premixed C<sub>5</sub>–C<sub>12</sub> *n*-alkane flames. Implementing innovative designs of high temperature, high pressure, and constant pressure combustion chamber environments and a nonlinear extrapolation method, Kelley et al. [11] determined the laminar flame velocities of C<sub>5</sub>–C<sub>8</sub> *n*-alkanes and air under high pressure and the high-fidelity experimental data of Markstein length from the propagation velocities of spark-ignited and expanding flames. Cheng et al. [12] investigated the laminar flame speeds of three pentene isomers and *n*-pentane through experiments and kinetic models. Rouso et al. [13] explored the chemical kinetics of low-temperature oxidation and pyrolysis of pentane under plasma-assisted conditions. In an atmospheric jet-stirred reactor, Zhao et al. [14] studied the low-temperature oxidation reaction of *n*-pentane by adding nitric oxide. Chen et al. [15] studied the co-pyrolytic mechanisms, kinetics, emissions, and products of sewage sludge and coffee grounds at 5 atm.

In summary, the current research is directed to the detailed mechanism of *n*-pentane, and the research on the simplified mechanism of *n*-pentane applied to CFD is very lacking. Since light hydrocarbon gas is mostly used for civilian combustion instead of natural gas, the simplified and optimized mechanism is only applicable to atmospheric pressure in this paper. The NUI Galway pentane isomer model (NUIG) is chosen in this paper based on Jiang et al.'s [9] research on different detailed mechanisms of *n*-pentane, including 697 species and 3214 reactions, and all simulation studies below have added gas transport file.

The main motivation of this paper is to simplify the detailed mechanism of *n*-pentane and further optimize the simplified mechanism. After obtaining the optimized mechanism, the combustion characteristic parameters predicted by the simplified mechanism and optimized mechanism of *n*-pentane, including the ignition delay time, laminar flame speed, species profile, and extinction residence time, are compared and discussed with the results predicted by the detailed mechanism and experimental data.

## 2. Simplified and Optimized Mechanism

All models used in this paper are provided by ANSYS CHEMKIN 17.0 [16]. The simplification of NUIG is based on the ignition delay time calculated by the closed homogeneous batch reactor

model, and is performed under the equivalence ratio of 1.0, and the temperatures of 1000 and 1600 K at the normal pressure. The ignition delay time is defined as the moment of autoignition. First, the Directed Relation Graph with Error Propagation and the Sensitivity Analysis (DRGEP/SA) [17] of ANSYS CHEMKIN 17.0 is used. The target parameter is the ignition delay time. The relative tolerance is set as 20% at the endpoint. The important species are chosen as  $n\text{-C}_5\text{H}_{12}$ ,  $\text{O}_2$ ,  $\text{N}_2$ ,  $\text{CO}_2$ ,  $\text{H}_2\text{O}$ ,  $\text{H}$ ,  $\text{O}$ , and  $\text{OH}$ . As a result, a skeletal mechanism, which is simplified by the DRGEP/SA method and referred to as DGPA for short, of 76 species and 448 reactions is obtained. Later, manual screening is performed based on the temperature sensitivity of NUIG, species change degree, and flow rate sensitivity of DGPA. Manual screening refers to the removal of unimportant species and corresponding reactions. Finally, a simplified mechanism, which is named as the mechanism of Hebei University of Engineering (HBUE), including 26 species and 134 reactions and an optimized mechanism, which is named as the mechanism of School of Energy and Environmental Engineering (SEEE), that optimizes the A-factor of the two reactions in HBUE are obtained. The experimental data of the ignition delay time of  $n$ -pentane in the temperature range of 1000–1100 K is not available, so it cannot be considered that the optimized mechanism is the most appropriate. The optimization process here is to provide a theoretical idea and basis for researchers who need to optimize the mechanism of  $n$ -pentane. The process of simplification and optimization is described in detail below.

### 2.1. DRGEP/SA

DRGEP/SA is divided into two-steps. The first step is based on the Directed Relation Graph with Error Propagation (DRGEP) method proposed by Pepiot-Desjardins and Pitsch [18], which in turn is an extension of the original Directed Relation Graph (DRG) method proposed by Lu and Law [19–21], and the second step is based on the Sensitivity Analysis (SA) of Zheng et al. [22].

The DRG method identifies species that are not important in the reaction mechanism by solving species coupling without any systematic knowledge. The direct species coupling is defined by the direct error in the production rate of one species,  $A$ , which is introduced by the removal of another species,  $B$ , from the mechanism. This direct error called  $r_{AB}$  can be expressed as:

$$r_{AB} \equiv \frac{\sum_{i=1,I} |v_{A,i} \omega_i \delta_{Bi}|}{\sum_{i=1,I} |v_{A,i} \omega_i|} \quad (1)$$

$$\delta_{Bi} = \begin{cases} 1, & \text{if the } i\text{th reaction involves species } B \\ 0, & \text{otherwise} \end{cases} \quad (2)$$

where  $A$  and  $B$  indicate the species,  $i$  indicates the  $i$ th reaction of the mechanism,  $v_{A,i}$  indicates the stoichiometric coefficient of species  $A$  in the  $i$ th reaction, and  $\omega_i$  is the reaction rate of the  $i$ th reaction.

The DRG method was extended to the DRGEP method. In DRGEP, once species  $A$  is kept in the mechanism, all other species that are reachable from species  $A$  through direct and indirect coupling are examined using their “ $R$ -value”, which is defined as:

$$R_A(B) = \max_S \{r_{ij}\} \quad (3)$$

where  $S$  is the set of all possible paths leading from species  $A$  to species  $B$ , and  $r_{ij}$  is the chain product of the weights (i.e., the direct error  $r_{ij}$ ) of the edges along the given path.

In the SA method, marginal species with the direct error above the final threshold  $\varepsilon_f$  but below a higher value  $\varepsilon_h$  need to be removed for analysis:

$$\varepsilon_f < R_A(B) < \varepsilon_h \quad (4)$$

Species with a direct error greater than  $\varepsilon_h$  are automatically retained in the skeletal mechanism:

$$R_A(B) > \varepsilon_h \quad (5)$$

First, remove marginal species that cause the ignition delay time error one by one from the mechanism and then sort in ascending order according to the following formula:

$$\delta_B = |\delta_{B,ind} - \delta_{DRGEP}| \quad (6)$$

where  $\delta_B$  is the induced error due to the removal of species  $B$  and  $\delta_{DRGEP}$  is the error of the DRGEP-generated mechanism.

## 2.2. Temperature Sensitivity

Temperature sensitivity analysis is carried out to identify the important and unimportant reactions at temperatures 1000 K, 1300 K, and 1600 K using the closed homogeneous batch reactor model, respectively. The normalized sensitivity coefficient ( $S_{k_i}$ ) of ignition delay time [23] is calculated by the following equation:

$$S_{k_i} = \frac{\tau(2k_i) - \tau(0.5k_i)}{2k_i - 0.5k_i} \cdot \frac{k_i}{\tau(k_i)} = \frac{\tau(2k_i) - \tau(0.5k_i)}{1.5(k_i)} \quad (7)$$

where  $\tau$  is the ignition delay time of the mixture of *n*-pentane/air and  $k_i$  is the rate coefficient of the *i*th reaction. The negative sensitivity coefficient indicates that the corresponding reaction suppresses the ignition delay time and promotes the ignition of the mixture, while the positive sensitivity coefficient indicates the opposite. Figure 1 shows the normalized sensitivity coefficients of ignition delay time of NUIG at an equivalent ratio of 1.0 and temperatures of 1000 K, 1300 K, and 1600 K, respectively. These reactions and species have a critical effect on the ignition delay time and must be retained in the subsequent simplified process. It is emphasized that  $2\text{HO}_2 = \text{H}_2\text{O}_2 + \text{O}_2$  (-1) and  $2\text{HO}_2 = \text{H}_2\text{O}_2 + \text{O}_2$  (-2) only have a suppressive effect on ignition at 1000 K, while  $n\text{-C}_5\text{H}_{12} + \text{HO}_2 = \text{C}_5\text{H}_{11-2} + \text{H}_2\text{O}_2$ ,  $n\text{-C}_5\text{H}_{12} + \text{HO}_2 = \text{C}_5\text{H}_{11-3} + \text{H}_2\text{O}_2$  and  $\text{H}_2\text{O}_2 (+\text{M}) = 2\text{OH} (+\text{M})$  only have a promotion effect at 1000 K, which lays the foundation for the subsequent mechanism optimization.

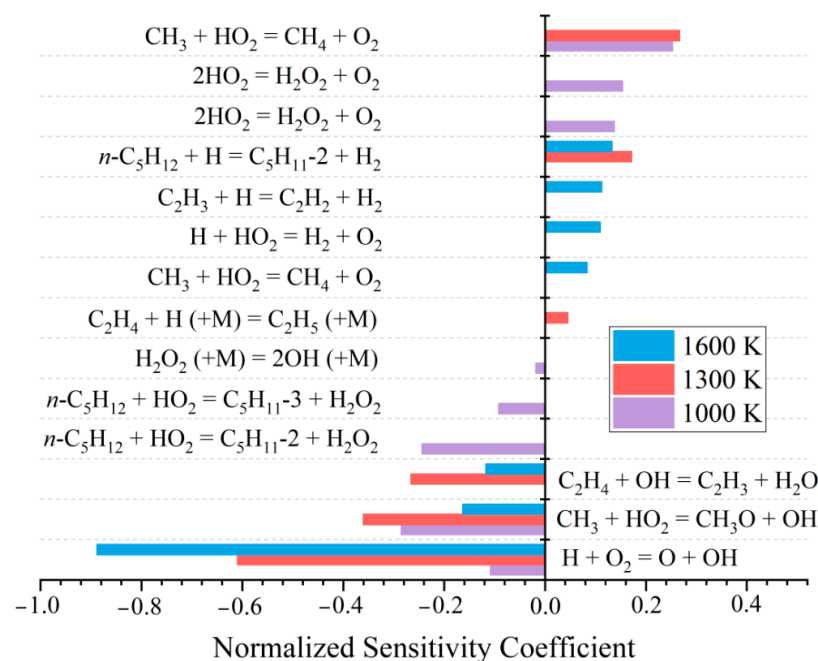


**Figure 1.** The normalized sensitivity coefficients of ignition delay time calculated with NUIG at an equivalent ratio of 1.0 and temperatures of 1000 K, 1300 K and 1600 K, respectively.

### 2.3. Species Change Degree

Species change degree can clearly reflect the formation and decomposition of each species in the chemical reaction. It can retain the species with a large degree of change and that play a key role, and remove unnecessary redundant species. The closed homogeneous batch reactor model is used. Figures 2–4 show the changes of species of DGPA when equivalence ratio is 1.0 and temperatures are 1000 K, 1300 K, and 1600 K, respectively. DGPA contains 76 species, and only the key 26 species remaining are shown in Figures 2–4.  $\text{CH}_3\text{O}$  and  $\text{C}_2\text{H}_3$  are not actually dominant in the chemical reaction, but they exist in  $\text{CH}_3 + \text{HO}_2 = \text{CH}_3\text{O} + \text{OH}$  and  $\text{C}_2\text{H}_4 + \text{OH} = \text{C}_2\text{H}_3 + \text{H}_2\text{O}$ , which are dominant for temperature, and play an important role in the ignition, so  $\text{CH}_3\text{O}$  and  $\text{C}_2\text{H}_3$  must be retained.

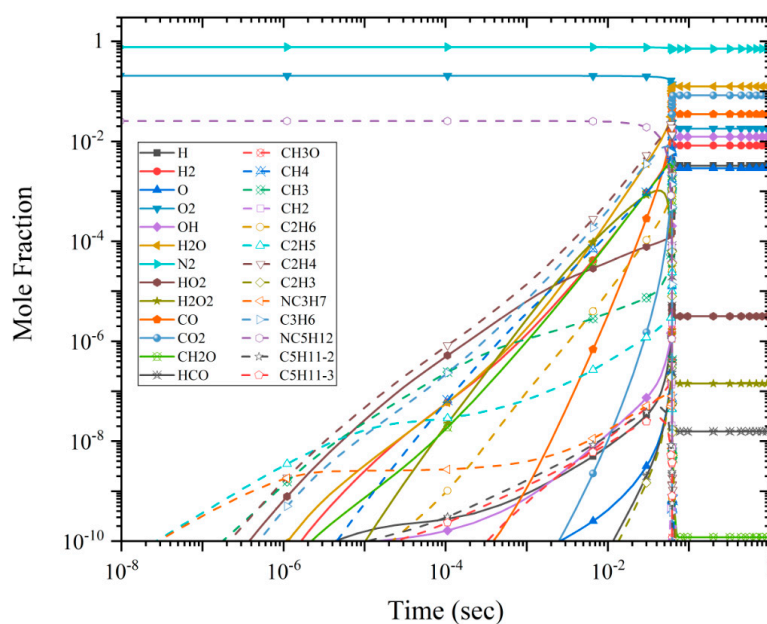


**Figure 2.** The changes of species calculated with DGPA at an equivalent ratio of 1.0 and a temperature of 1000 K.

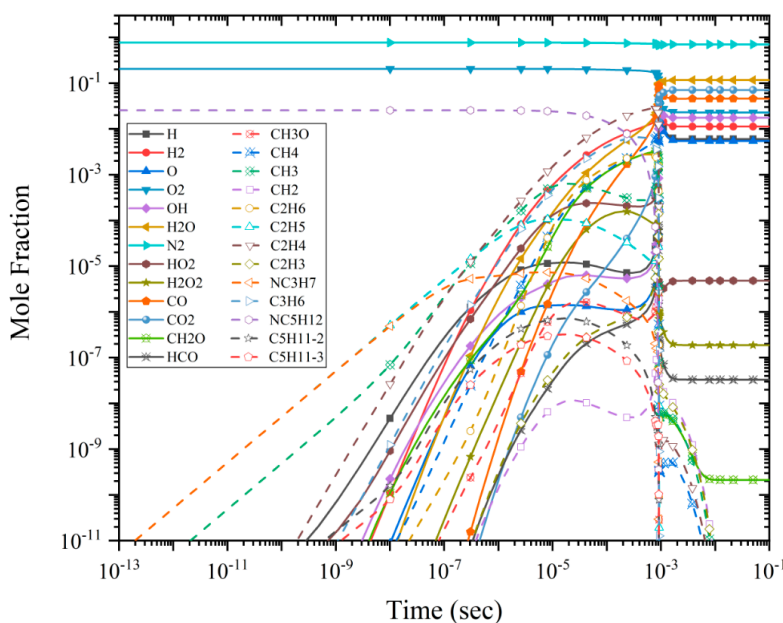


**Figure 3.** The changes of species calculated with DGPA at an equivalent ratio of 1.0 and a temperature of 1300 K.



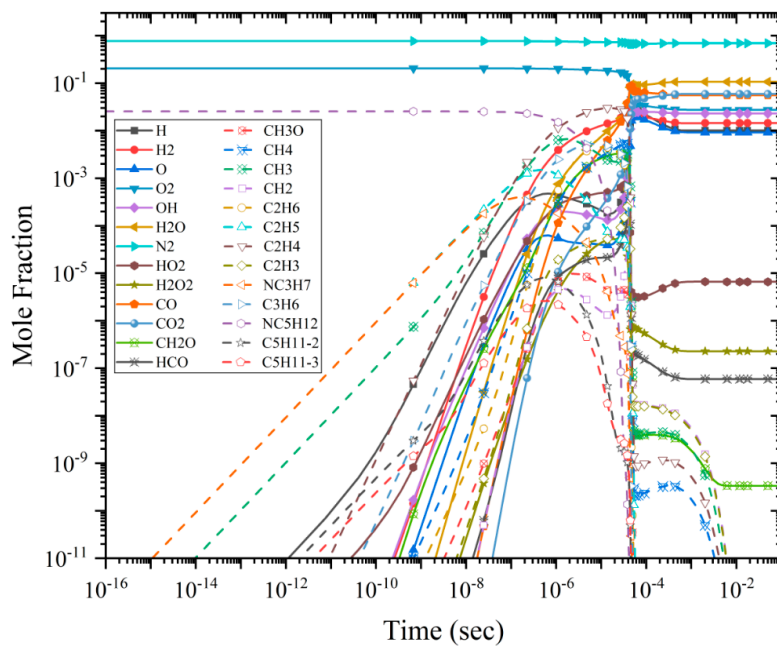


**Figure 4.** The changes of species calculated with DGPA at an equivalent ratio of 1.0 and a temperature of 1600 K.

#### 2.4. Flow Rate Sensitivity

The characteristic chemical reaction of laminar flame speed needs to be simplified through selection of flow rate sensitivity analysis. The premixed laminar flame-speed calculation model is used in this part. Figure 5 shows the flow rate sensitivity coefficients of laminar flame speed of DGPA at an unburned gas temperature of 298 K and equivalent ratios of 0.6–1.7. The chemical reactions in the legend of Figure 5 are shown in Table 1. Only 14 reactions have great influence on the laminar flame speed. The reactions related to the species that are not retained in the species change analysis are all removed, and the comparison with the detailed mechanism shows that there is no effect.

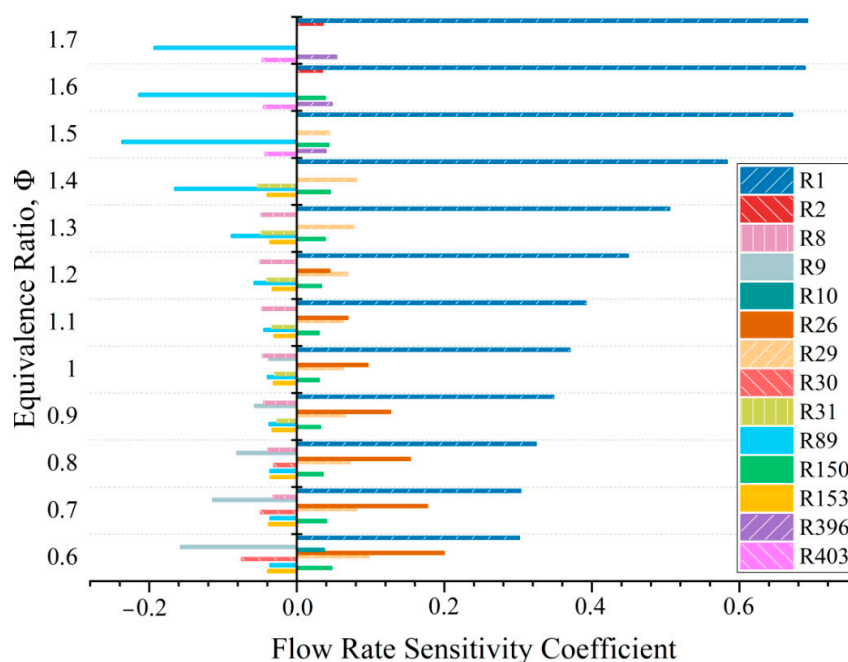


**Figure 5.** The flow rate sensitivity coefficients of laminar flame speed calculated with DGPA at an unburned gas temperature of 298 K and equivalent ratios of 0.6–1.7.

**Table 1.** The chemical reactions in the legend of Figure 5.

| Number | Reaction                   | Number | Reaction                              |
|--------|----------------------------|--------|---------------------------------------|
| R1     | $H + O_2 = O + OH$         | R30    | $HCO + O_2 = CO + HO_2$               |
| R2     | $O + H_2 = H + OH$         | R31    | $HCO + H = CO + H_2$                  |
| R8     | $H + OH + M = H_2O + M$    | R89    | $CH_3 + H (+M) = CH_4 (+M)$           |
| R9     | $H + O_2 (+M) = HO_2 (+M)$ | R150   | $C_2H_4 + H (+M) = C_2H_5 (+M)$       |
| R10    | $HO_2 + H = 2OH$           | R153   | $2CH_3 = H + C_2H_5$                  |
| R26    | $CO + OH = CO_2 + H$       | R396   | $n-C_5H_{12} = n-C_3H_7 + C_2H_5$     |
| R29    | $HCO + M = H + CO + M$     | R403   | $n-C_5H_{12} + H = C_5H_{11-3} + H_2$ |

### 2.5. Optimization Analysis

After removing the unimportant species and reactions through the above steps, a simplified mechanism (HBUE) including 26 species and 134 reactions is obtained. The experimental data of Bugler et al. [7] on the ignition delay time for *n*-pentane/air mixtures at an equivalence ratio of 1.0 were presented. Figure 6 shows the ignition delay times calculated using NUIG, DGPA, HBUE, SEEE and the experimental data at an equivalence ratio of 1.0. Compared with NUIG, the average error of the ignition delay time of HBUE is 14.01%, but the maximum error of temperature reached 72.30% at 1000 K. The errors of ignition delay at 1063 K and 1095 K are 29.31% and 14.89%, respectively. Therefore, the optimization is mainly at 1000–1100 K. Table 2 shows the two reactions that need to be optimized in the simplified mechanism. An optimized mechanism (SEEE) can be obtained by reducing the A-factor of  $2HO_2 = H_2O_2 + O_2$  (−1) and  $2HO_2 = H_2O_2 + O_2$  (−2) by 10 times. In the temperature sensitivity analysis, the effects of  $2HO_2 = H_2O_2 + O_2$  (−1) and  $2HO_2 = H_2O_2 + O_2$  (−2),  $n-C_5H_{12} + HO_2 = C_5H_{11-2} + H_2O_2$ ,  $n-C_5H_{12} + HO_2 = C_5H_{11-3} + H_2O_2$  and  $H_2O_2 (+M) = 2OH (+M)$  on temperature have been mentioned, but, after testing,  $n-C_5H_{12} + HO_2 = C_5H_{11-2} + H_2O_2$ ,  $n-C_5H_{12} + HO_2 = C_5H_{11-3} + H_2O_2$ , and  $H_2O_2 (+M) = 2OH (+M)$  have a greater impact on the ignition delay time, and the optimized results are not as good as  $2HO_2 = H_2O_2 + O_2$  (−1) and  $2HO_2 = H_2O_2 + O_2$  (−2). It can be clearly seen from Figure 6 that the ignition delay time of SEEE and NUIG are in better agreement overall, especially at 1000–1100 K, and the average error and the maximum error of SEEE compared with NUIG are 11.25% and 19.57%, respectively. It is emphasized again that, due to the lack of experimental data at 1000–1100 K, SEEE is based on the optimization of HBUE, and the error is smaller than that of NUIG. The optimized process provides a good reference for future research on the mechanism of *n*-pentane.

**Table 2.** Optimized reactions from HBUE to SEEE.

|      | Reactions                   | $A_i$                 | $\beta_i$ | $E_i$    |
|------|-----------------------------|-----------------------|-----------|----------|
| HBUE | $2HO_2 = H_2O_2 + O_2$ (−1) | $1 \times 10^{14}$    | 0.0       | 11,040.9 |
|      | $2HO_2 = H_2O_2 + O_2$ (−2) | $1.90 \times 10^{11}$ | 0.0       | −1408.9  |
| SEEE | $2HO_2 = H_2O_2 + O_2$ (−1) | $1 \times 10^{13}$    | 0.0       | 11,040.9 |
|      | $2HO_2 = H_2O_2 + O_2$ (−2) | $1.90 \times 10^{10}$ | 0.0       | −1408.9  |



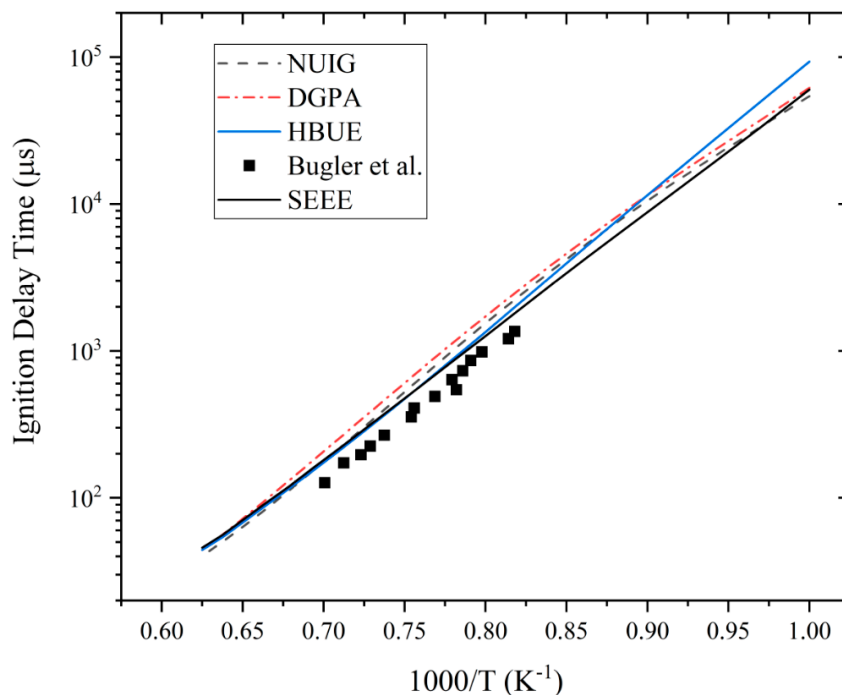


**Figure 6.** Comparison of the ignition delay times between NUIG, DGPA, HBUE, SEEE, and experimental data at an equivalence ratio of 1.0.

### 3. Verification and Discussion

#### 3.1. Ignition Delay Time

The experimental data of Bugler et al. of the ignition delay time for *n*-pentane/air mixtures at equivalence ratios of 0.3, 0.5, and 2.0 measured using the shock tube were presented [7]. Figures 6–9 show the ignition delay times calculated using NUIG, DGPA, HBUE, SEEE, and the experimental data at temperatures of 1000–1600 K. The error analysis of Figure 6 is detailed in Section 2.4. Figure 7 shows the ignition delay times calculated using NUIG, DGPA, HBUE, SEEE, and the experimental data at an equivalence ratio of 0.3. Compared with NUIG, the average errors of HBUE and SEEE are 34.83% and 55.86%, respectively, and their corresponding maximum errors are 84.55% and 70.91%, respectively. Figure 8 shows the ignition delay times calculated using NUIG, DGPA, HBUE, SEEE, and the experimental data at an equivalence ratio of 0.5. Compared with NUIG, the average errors of HBUE and SEEE are 17.97% and 19.97%, respectively, and the maximum errors of them are 74.60% and 27.99%, respectively. Figure 9 shows the ignition delay times calculated using NUIG, DGPA, HBUE, SEEE, and the experimental data at an equivalence ratio of 2.0. Compared with NUIG, the average errors of HBUE and SEEE are 16.42% and 18.60%, respectively, and their corresponding maximum errors are 77.83% and 33.53%, respectively. In general, with the increase of the equivalence ratio, the variation curve of the ignition delay time of HBUE and SEEE with temperature shifts to near the NUIG and experimental data. That is to say, the ignition delay times predicted by SEEE at equivalence ratios of 0.5 to 2.0 are in good agreement with NUIG and experimental data, and the prediction of HBUE at 1100–1600 K is also good.

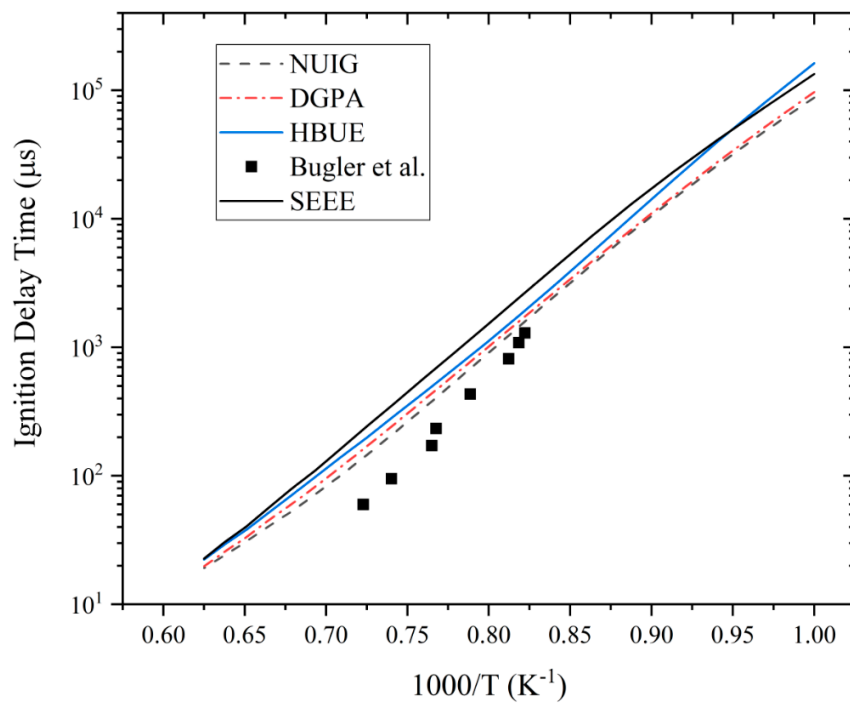


**Figure 7.** Comparison of the ignition delay times between NUIG, DGPA, HBUE, SEEE, and experimental data at an equivalence ratio of 0.3.

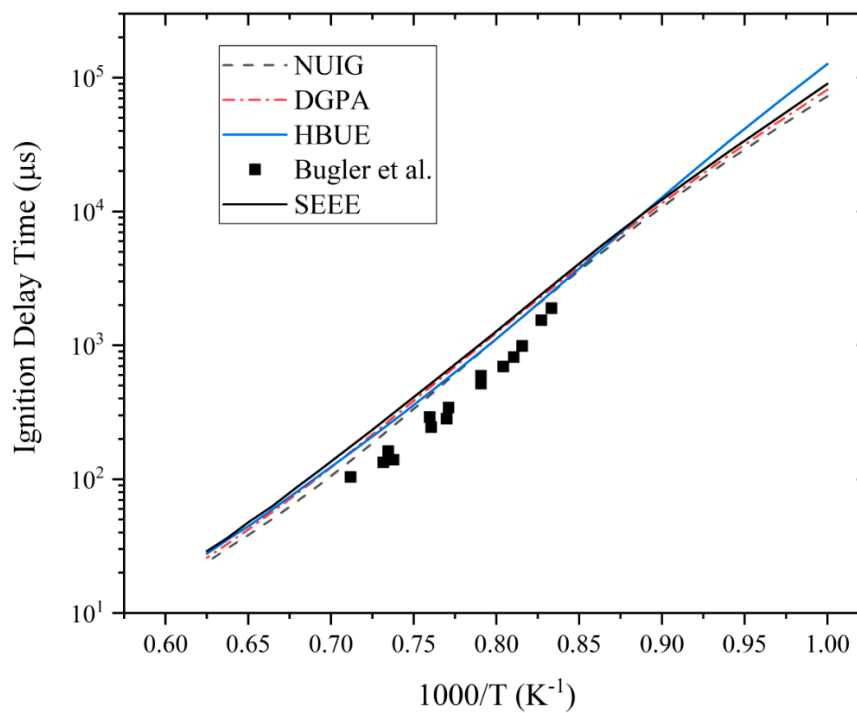


**Figure 8.** Comparison of the ignition delay times between NUIG, DGPA, HBUE, SEEE, and experimental data at an equivalence ratio of 0.5.

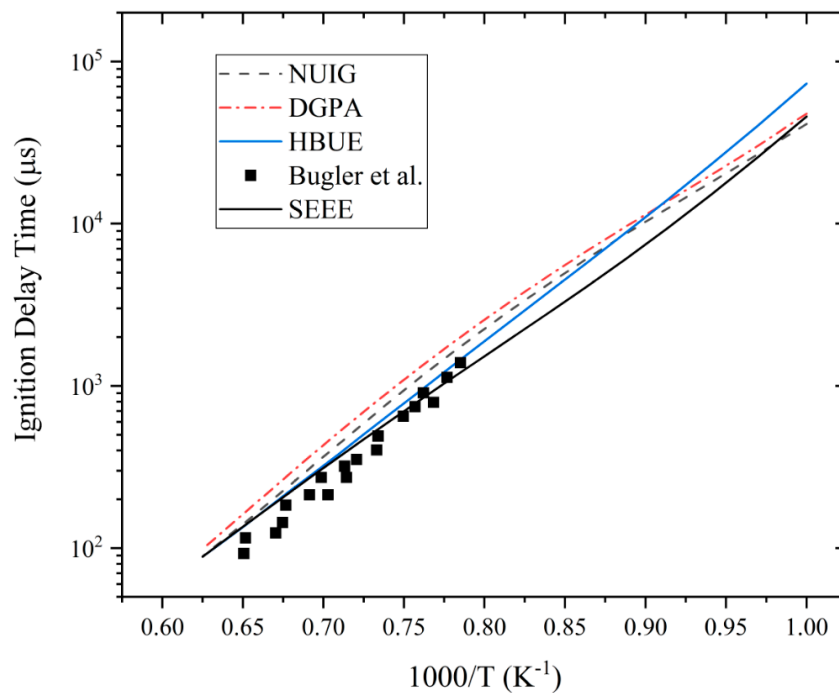


**Figure 9.** Comparison of the ignition delay times between NUIG, DGPA, HBUE, SEEE, and experimental data at an equivalence ratio of 2.0.

### 3.2. Laminar Flame Speed

Civil light hydrocarbon gas is usually burned at room temperature; therefore, the laminar flame speed of HBUE and SEEE is compared with NUIG and experimental data at an unburned gas temperature of 353 K, and with NUIG only at 298 K. Experimental data on the laminar flame speed of *n*-pentane/air mixtures at equivalence ratios of 0.6–1.7 and an unburned gas temperature of 353 K were determined by Kelley et al. [11]. Figure 10 presents the premixed laminar flame speeds calculated with NUIG, DGPA, HBUE, SEEE, and the experimental data. Compared with NUIG, the average errors of HBUE and SEEE are 5.28% and 4.98%, respectively, and their maximum errors are 23.21% and 21.68%, respectively, with an equivalent ratio of 1.7. Figure 11 shows the comparison of NUIG, DGPA, HBUE, and SEEE for predicting the laminar flame speeds at an unburned gas temperature of 298 K. Compared with NUIG, the average errors of HBUE and SEEE are 5.91% and 5.98%, respectively, and their maximum errors are 26.28% and 25.58%, respectively, with an equivalent ratio of 1.7. At two unburned gas temperatures, at each equivalent ratio, except 1.7, the laminar flame speed predicted by HBUE and SEEE is quite consistent with NUIG.

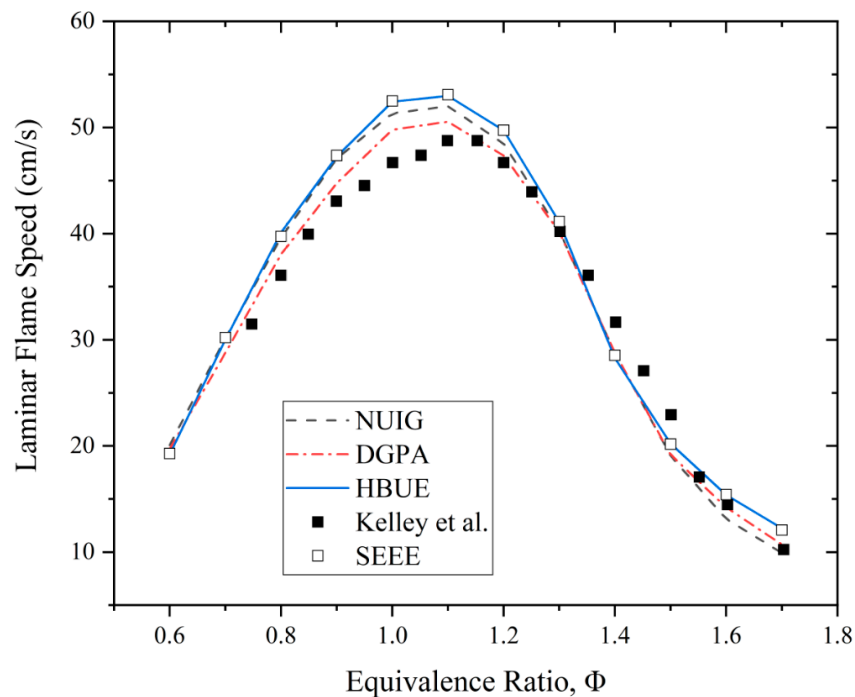


**Figure 10.** Comparison of the laminar flame speeds between NUIG, DGPA, HBUE, SEEE, and experimental data at equivalence ratios of 0.6–1.7 and an unburned gas temperature of 353 K.

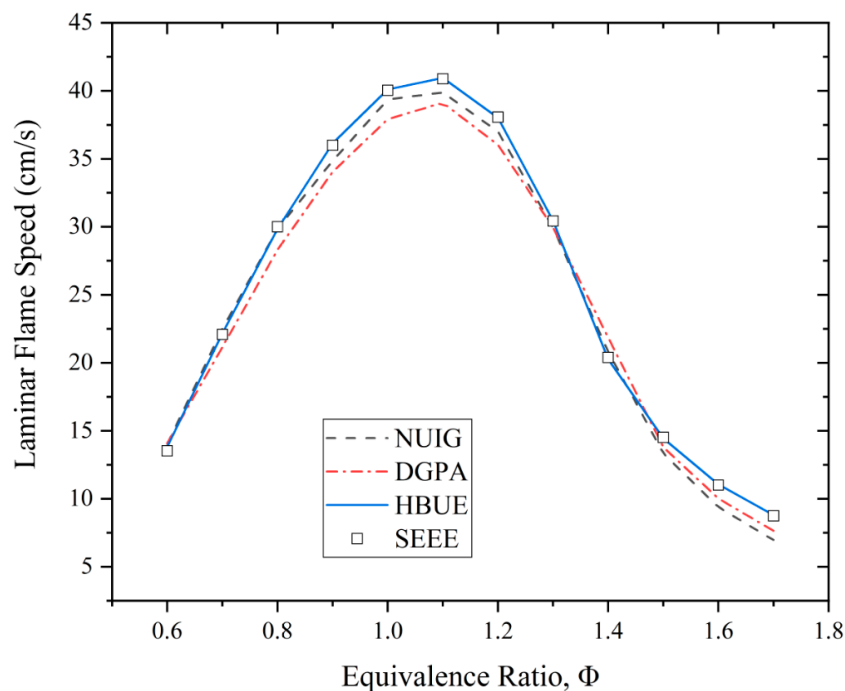


**Figure 11.** Comparison of the laminar flame speeds between NUIG, DGPA, HBUE, and SEEE at equivalence ratios of 0.6–1.7 and an unburned gas temperature of 298 K.

### 3.3. Species Mole Fraction

Species profiles are simulated using the premixed laminar burner-stabilized flame model with the mechanisms of NUIG, DGPA, HBUE, and SEEE at an equivalence ratio of 1.0 and an unburned gas temperature of 298 K. Figure 12 shows the concentration profiles of some key  $C_1$ – $C_3$  species, and Figure 13 shows the corresponding profiles for some key oxidation species involving H, O, OH, and CO. The predicted concentration of the key  $C_1$ – $C_3$  species with HBUE and SEEE is higher than

that of NUIG as shown in Figure 12, but the overall change trend is consistent. This error can be expected due to the reduction of species in HBUE and SEEE, and the decomposition pathways of  $C_1$ – $C_3$  is different from that of NUIG. However, the concentration of smaller oxidation radicals is nearly identical, as shown in Figure 13.

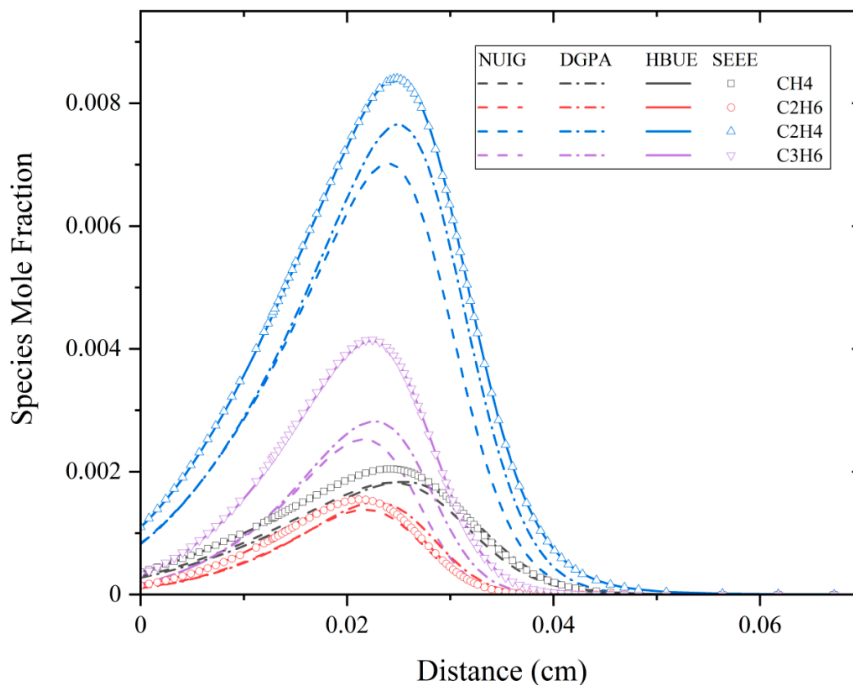


**Figure 12.** Comparison of the mole fraction for the key  $C_1$  to  $C_3$  species between NUIG, DGPA, HBUE, and SEEE for burner-stabilized flame at an equivalence ratio of 1.0 and an unburned gas temperature of 298 K.

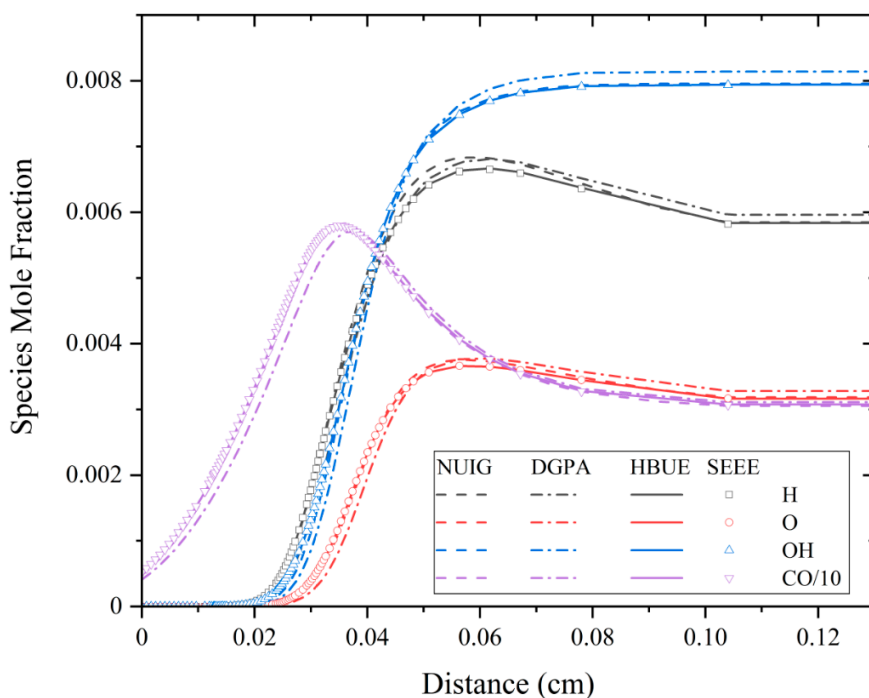


**Figure 13.** Comparison of the mole fraction for the key oxidation species between NUIG, DGPA, HBUE, and SEEE for burner-stabilized flame at an equivalence ratio of 1.0 and an unburned gas temperature of 298 K.

### 3.4. Extinction Residence Time

The extinction residence time [24,25] is an important parameter for verifying the performance of the chemical reaction mechanism. The perfectly stirred reactor (PSR) is used to determine the extinction limit by reducing the residence time until there is insufficient time to react. Figure 14 shows the relationship curves (C-curves) of the residence time and the temperature at an equivalent ratio of 1.0 and an initial temperature of 298 K calculated with NUIG, DGPA, HBUE, and SEEE. Compared with NUIG, the average errors of the temperatures predicted by HBUE and SEEE at different residence times are 0.30% and 0.25%, respectively, and their maximum errors are 1.77% and 0.79%, respectively. The extinction temperature is defined as the characteristic temperature corresponding to the extinction residence time. According to the C-curve, each residence time corresponds to two temperatures, but the extinction limit only corresponds to one temperature. The extinction residence times calculated with NUIG, DGPA, HBUE, and SEEE are very close; therefore, the extinction temperature is used for comparison and verification. Figure 15 shows the extinction temperatures predicted by NUIG, DGPA, HBUE, and SEEE at equivalent ratios of 0.5–1.6. Compared with NUIG, the average errors of HBUE and SEEE are 0.61% and 0.60%, respectively, and their maximum errors are 1.15% and 1.15%, respectively. This indicates that HBUE and SEEE still have a very good performance in the prediction of unsteady combustion.

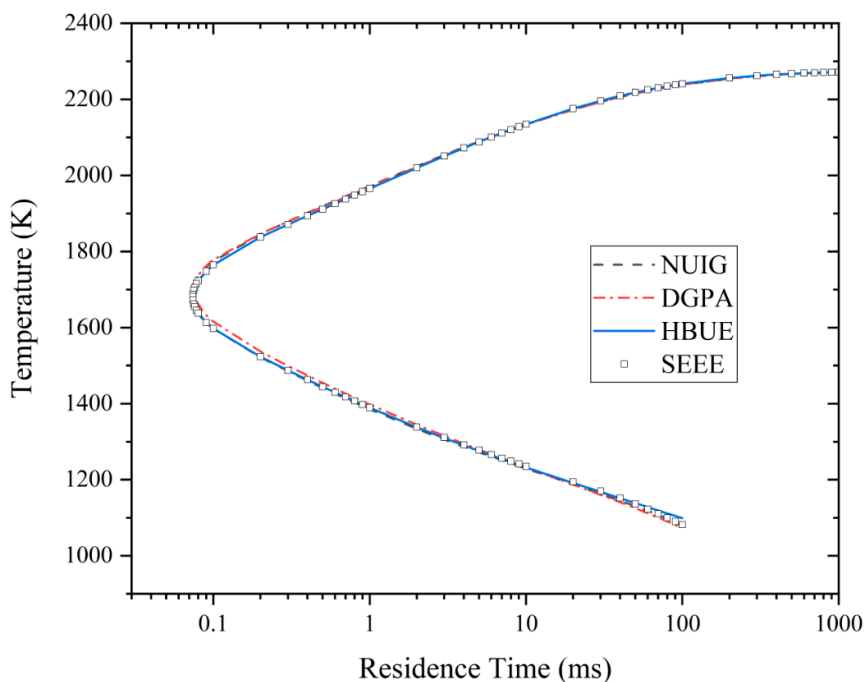


**Figure 14.** Comparison of C-curves between NUIG, DGPA, HBUE, and SEEE at an equivalence ratio of 1.0 and an initial temperature of 298 K.



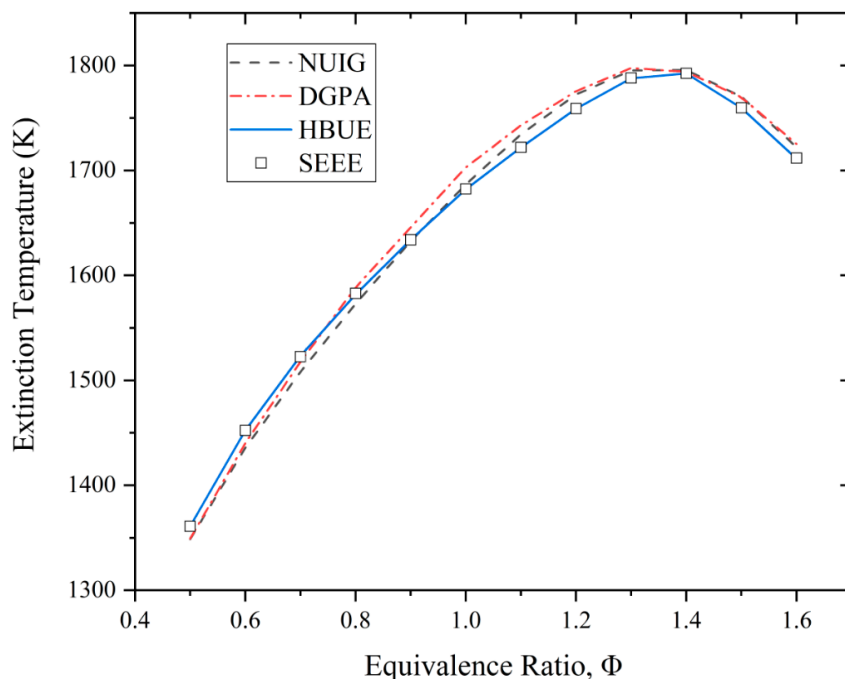


**Figure 15.** Comparison of the extinction temperatures between NUIG, DGPA, HBUE, and SEEE at equivalence ratios of 1.0 and an initial temperature of 298 K.

#### 4. Conclusions

Currently, there is no simplified mechanism for combustion of *n*-pentane, which is the main component of civil light hydrocarbon gas. In this work, a detailed mechanism of *n*-pentane, including 697 species and 3214 reactions, is simplified to a mechanism with 26 species and 134 reactions at normal pressure, combining the methods of DRGEPSSA, temperature sensitivity, species change degree, and flow rate sensitivity. Based on the temperature sensitivity analysis, the two chemical reactions  $2\text{HO}_2 = \text{H}_2\text{O}_2 + \text{O}_2$  (−1) and  $2\text{HO}_2 = \text{H}_2\text{O}_2 + \text{O}_2$  (−2) are optimized to greatly improve the accuracy in the temperature range of 1000–1100 K. Then, in terms of the characteristic parameters of ignition delay time, laminar flame speed, species profile, and extinction residence time, the simplified mechanism and optimized mechanism are compared with the detailed mechanism and experimental data. The results indicate that in the temperature range of 1100–1600 K, the simplified mechanism and the optimized mechanism have a good agreement, while in the temperature range of 1000–1100 K, compared with the simplified mechanism, the accuracy of the optimized mechanism is higher. Due to the lack of experimental data of the ignition delay time in the temperature range of 1000–1100 K, the optimized mechanism is not necessarily the optimal mechanism. However, this requires in-depth experimental research under the corresponding working conditions, which is the content of our work in the future.

**Author Contributions:** Conceptualization, Z.M.; Methodology, Z.M.; Validation, J.W.; Formal analysis, Z.M., J.Q. and C.X.; Resources, J.W.; Writing—original draft preparation, Z.M.; Writing—review and editing, Z.M. and J.W.; Data curation, J.Q., L.H. and J.L.; Visualization, Z.M.; Software, Z.M.; Supervision, C.X., J.Q. and J.L.; Project administration, J.W. and L.H.; Funding acquisition, J.W. All authors have read and agreed to the published version of the manuscript.

**Funding:** This work was supported by the Central Government of China Guides Special Foundation for Local Science and Technology Development (19944508G).

**Acknowledgments:** NUI Galway pentane isomer model was shared by National University of Ireland, Galway.

**Conflicts of Interest:** The authors declare no conflict of interest.

## References

1. Wen, F.; Zhong, B. Skeletal Mechanism Generation Based on Eigenvalue Analysis Method. *Acta Phys.-Chim. Sin.* **2012**, *28*, 1306–1312.
2. Meng, Z.; Wang, J.; Xiong, C.; Qi, J.; Hou, L. Research on Combustion Characteristics of Air–Light Hydrocarbon Mixing Gas. *Processes* **2020**, *8*, 730. [[CrossRef](#)]
3. Knox, J.H.; Kinnear, C. The mechanism of combustion of pentane in the gas phase between 250 and 400 C. *Symp. (Int.) Combust.* **1971**, *13*, 217–227. [[CrossRef](#)]
4. Hughes, R.; Simmons, R. The low-temperature combustion of n-pentane. *Symp. (Int.) Combust.* **1969**, *12*, 449–461. [[CrossRef](#)]
5. Westbrook, C.K.; Pitz, W.J.; Thornton, M.M.; Malte, P.C. A kinetic modeling study of n-pentane oxidation in a well-stirred reactor. *Combust. Flame* **1988**, *72*, 45–62. [[CrossRef](#)]
6. Chakir, A.; Belumam, M.; Boettner, J.; Cathonnet, M. Kinetic study of n-pentane oxidation. *Combust. Sci. Technol.* **1991**, *77*, 239–260. [[CrossRef](#)]
7. Bugler, J.; Marks, B.; Mathieu, O.; Archuleta, R.; Camou, A.; Grégoire, C.; Heufer, K.A.; Petersen, E.L.; Curran, H.J. An ignition delay time and chemical kinetic modeling study of the pentane isomers. *Combust. Flame* **2016**, *163*, 138–156. [[CrossRef](#)]
8. Zhukov, V.; Sechenov, V.; Starikovskii, A.Y. Self-ignition of a lean mixture of n-pentane and air over a wide range of pressures. *Combust. Flame* **2005**, *140*, 196–203. [[CrossRef](#)]
9. Jiang, X.; Deng, F.; Yang, F.; Zhang, Y.; Huang, Z. High temperature ignition delay time of DME/n-pentane mixture under fuel lean condition. *Fuel* **2017**, *191*, 77–86. [[CrossRef](#)]
10. Ji, C.; Dames, E.; Wang, Y.L.; Wang, H.; Egolfopoulos, F.N. Propagation and extinction of premixed C5–C12 n-alkane flames. *Combust. Flame* **2010**, *157*, 277–287. [[CrossRef](#)]
11. Kelley, A.; Smallbone, A.; Zhu, D.; Law, C.K. Laminar flame speeds of C5 to C8 n-alkanes at elevated pressures: Experimental determination, fuel similarity, and stretch sensitivity. *Proc. Combust. Inst.* **2011**, *33*, 963–970. [[CrossRef](#)]
12. Cheng, Y.; Hu, E.; Lu, X.; Li, X.; Gong, J.; Li, Q.; Huang, Z. Experimental and kinetic study of pentene isomers and n-pentane in laminar flames. *Proc. Combust. Inst.* **2017**, *36*, 1279–1286. [[CrossRef](#)]
13. Rousso, A.; Mao, X.; Chen, Q.; Ju, Y. Kinetic studies and mechanism development of plasma assisted pentane combustion. *Proc. Combust. Inst.* **2019**, *37*, 5595–5603. [[CrossRef](#)]
14. Zhao, H.; Wu, L.; Patrick, C.; Zhang, Z.; Rezgui, Y.; Yang, X.; Wysocki, G.; Ju, Y. Studies of low temperature oxidation of n-pentane with nitric oxide addition in a jet stirred reactor. *Combust. Flame* **2018**, *197*, 78–87. [[CrossRef](#)]
15. Chen, J.; Zhang, J.; Liu, J.; He, Y.; Evrendilek, F.; Buyukada, M.; Xie, W.; Sun, S. Co-pyrolytic mechanisms, kinetics, emissions and products of biomass and sewage sludge in N<sub>2</sub>, CO<sub>2</sub> and mixed atmospheres. *Chem. Eng. J.* **2020**, *397*, 125372. [[CrossRef](#)]
16. Chemkin, A.N.S.Y.S. 17.0 (15151); ANSYS Reaction Design: San Diego, CA, USA, 2016.
17. Niemeyer, K.E.; Sung, C.-J.; Raju, M.P. Skeletal mechanism generation for surrogate fuels using directed relation graph with error propagation and sensitivity analysis. *Combust. Flame* **2010**, *157*, 1760–1770. [[CrossRef](#)]
18. Pepiot-Desjardins, P.; Pitsch, H. An efficient error-propagation-based reduction method for large chemical kinetic mechanisms. *Combust. Flame* **2008**, *154*, 67–81. [[CrossRef](#)]
19. Lu, T.; Law, C.K. A directed relation graph method for mechanism reduction. *Proc. Combust. Inst.* **2005**, *30*, 1333–1341. [[CrossRef](#)]
20. Lu, T.; Law, C.K. On the applicability of directed relation graphs to the reduction of reaction mechanisms. *Combust. Flame* **2006**, *146*, 472–483. [[CrossRef](#)]
21. Lu, T.; Law, C.K. Linear time reduction of large kinetic mechanisms with directed relation graph: N-Heptane and iso-octane. *Combust. Flame* **2006**, *144*, 24–36. [[CrossRef](#)]
22. Zheng, X.; Lu, T.; Law, C.K. Experimental counterflow ignition temperatures and reaction mechanisms of 1, 3-butadiene. *Proc. Combust. Inst.* **2007**, *31*, 367–375. [[CrossRef](#)]
23. Hui, X.; Zhang, C.; Xia, M.; Sung, C.-J. Effects of hydrogen addition on combustion characteristics of n-decane/air mixtures. *Combust. Flame* **2014**, *161*, 2252–2262. [[CrossRef](#)]

24. Chang, L.; Lin, Y.; Cao, Z.; Xu, L. A new simplified mechanism for combustion of RP-3/Jet-A kerosene. *Energy Sources Part A* **2020**, *42*, 676–687. [[CrossRef](#)]
25. Chang, L.; Lin, Y.; Cao, Z.; Xu, L. Effects of water vapor addition on NO reduction of n-decane/air flames. *Energy Sources Part A* **2020**, *42*, 1526–1540. [[CrossRef](#)]



© 2020 by the authors. Licensee MDPI, Basel, Switzerland. This article is an open access article distributed under the terms and conditions of the Creative Commons Attribution (CC BY) license (<http://creativecommons.org/licenses/by/4.0/>).